

# Investigating the Formation of “Molybdenum Blues” with Gel Electrophoresis and Mass Spectrometry

Ippei Nakamura,<sup>†</sup> Haralampos N. Miras,<sup>§</sup> Aya Fujiwara,<sup>‡</sup> Masaru Fujibayashi,<sup>‡</sup> Yu-Fei Song,<sup>||</sup> Leroy Cronin,<sup>\*,§</sup> and Ryo Tsunashima<sup>\*,†</sup>

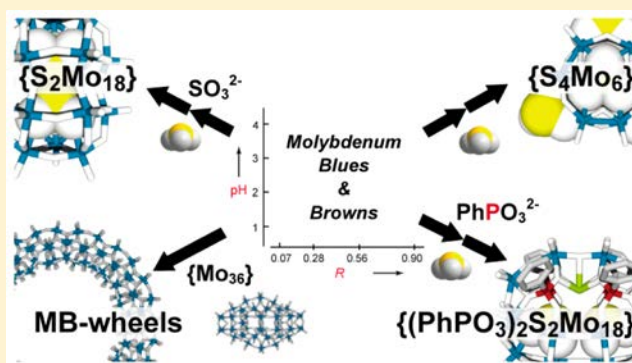
<sup>†</sup>Graduate School of Science and Engineering and <sup>‡</sup>Department of Biology and Chemistry, Yamaguchi University, Yamaguchi, 753 8512, Japan

<sup>§</sup>School of Chemistry, University of Glasgow, Glasgow G12 8QQ, United Kingdom

<sup>||</sup>State Key Laboratory of Chemical Resource Engineering, Beijing University of Chemical Technology, 100029 Beijing, P. R. China

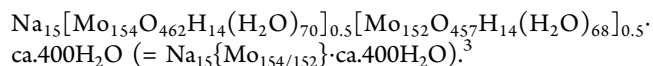
## S Supporting Information

**ABSTRACT:** The reduction of solutions of acidified molybdate leads to the formation of a family of nanostructured molybdenum blue (MB) wheels which are linked together in a series of complex reaction networks. These networks are complex because the species which define the nodes are extremely labile, unstable, and common to many different networks. Herein, we combine gel electrophoresis and electrospray ionization mass spectrometry (ESI-MS) to investigate the effect of the pH and the ratio of reactants and reducing agents,  $R$  ( $R = [\text{S}_2\text{O}_4^{2-}]/[\text{MoO}_4^{2-}]$ ), on the complex underlying set of equilibria that make up MBs. By mapping the reaction parameter space given by experimental variables such as pH,  $R$ , solvent medium, and type of counterion, we show that the species present range from nanostructured MB wheels (comprising ca. 154 Mo atoms) to smaller molecular capsules,  $[(\text{SO}_3)_2\text{Mo}^{\text{V}}_2\text{Mo}^{\text{VI}}_{16}\text{O}_{54}]^{6-}$  ( $\{\text{S}_2\text{Mo}_{18}\}$ ), and templated hexameric  $[(\mu_6\text{-SO}_3)\text{Mo}^{\text{V}}_6\text{O}_{15}(\mu_2\text{-SO}_3)_3]^{8-}$  ( $\{\text{S}_4\text{Mo}_6\}$ ) anions. The parallel effects of templation and reduction on the self-assembly process are discussed, taking into consideration the Lewis basicity of the template, the oxidation state of the Mo centers, and the polarity of the reaction medium. Finally, we report a new type of molecular cage (TBA)<sub>5</sub>[Na(SO<sub>3</sub>)<sub>2</sub>(PhPO<sub>3</sub>)<sub>4</sub>Mo<sup>V</sup><sub>4</sub>Mo<sup>VI</sup><sub>14</sub>O<sub>49</sub>] $\cdot n\text{MeCN}$  (**1**), templated by  $\text{SO}_3^{2-}$  anions and decorated by organic ligands. This discovery results from the exploration of the cooperative effect of two anions possessing comparable Lewis basicity, and we believe this constitutes a new synthetic approach for the design of new nanostructured molecular metal oxides and will lead to a greater understanding of the complex reaction networks underpinning the assembly of this family of nanoclusters.



## 1. INTRODUCTION

Solutions of molybdenum blues (MBs),<sup>1</sup> first mentioned by Scheele in 1783, comprise a family of nanostructured polyoxometalate (POM) clusters<sup>2</sup> where their deep-blue color originates from the partial reduction of  $\text{Mo}^{\text{VI}}$  centers to  $\text{Mo}^{\text{V}}$  giving a delocalized mixed valence state. Their preparation is achieved by the partial reduction of solutions of acidified molybdate(VI). Crystallization of the solutions lead to isolation of particular species, the nature of which is precisely defined by the pH of the reaction mixture. Specifically, acidification of  $\text{Na}_2\text{MoO}_4$  aqueous solution (12.7 mM, 25 mL) with hydrochloric acid (32%, 2.7 mL, results in solution pH  $\approx$  1) and consecutive reduction by  $\text{Na}_2\text{S}_2\text{O}_4$  (0.15 g, 0.86 mmol) leads to the formation of a nanostructured, wheel-shaped, Mo-oxide cluster composed of 154 (152) Mo atoms bridged by O atoms after 1–2 days. The mixed valence wheel is reduced by 28 electrons with a formula of



The structure can be rationalized simply by grouping the individual metal-centered units into building blocks, namely:  $14 \times$  each of  $\{\text{Mo}_1\}$ ,  $\{\text{Mo}_2\}$ , and  $\{\text{Mo}_8\}$  (Figure 1). Furthermore, the controlled elimination of  $\{\text{Mo}_2\}$  building units leads to the formation of similar wheels with “defect” sites where the wheel is formulated as  $\{\text{Mo}_{154-x}\}$  ( $x = 0-16$ ).

This family of compounds does attract attention due to their structural complexity and their interesting behavior in solution. For example, Liu et al. revealed that the  $\{\text{Mo}_{154/152}\}$  wheels form assemblies that have a vesicle-like or “blackberry” structure in solution even though they do not possess amphiphilic characteristics, which are often crucial for the formation of such assemblies. Investigation of the systems

Received: December 15, 2014

Published: April 21, 2015

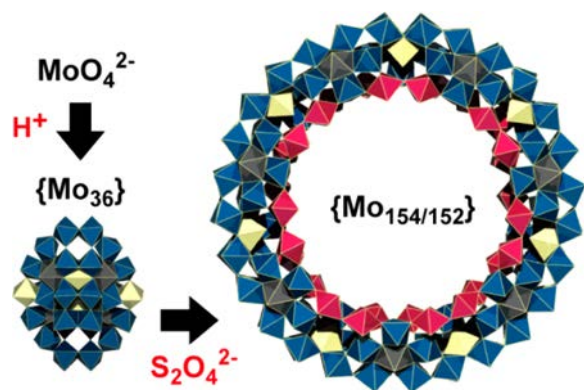


**Figure 1.** Schematic view of the formation of the  $\{\text{Mo}_{154/152}\}$  wheel. The polyhedral building blocks are colored as follows:  $\{\text{Mo}_1\}$ , yellow;  $\{\text{Mo}_2\}$ , red;  $\{\text{Mo}_8\}$ , blue with a black pentagonal central group.

reveals that the electrostatic interactions between the clusters and counterions are necessary for the formation of vesicles.<sup>4</sup> Additionally, a variety of applications, owing to the reactivity of the nanowheel, was proposed in areas such as catalysis, ion conduction, and host–guest chemistry.<sup>5</sup> Apart from these interesting properties, the complex formation mechanism attracted the attention of several research groups. Recently, the use of continuous flow reactors allowed the controlled reduction of the reaction mixture, giving the opportunity to isolate and characterize crystallographically an intermediate species of the MB family where the  $\{\text{Mo}_{36}\}$  cluster templates the formation of the MB wheel (Figure 1).<sup>6</sup>

In general, isolation of POM clusters has been achieved by crystallization, which requires precise control of both reaction and crystallization conditions as well as appropriate selection of cations and solvents. Occasionally, the inability to isolate single crystals from a reaction mixture leads to ambiguity with respect to the structure of the compound(s) isolated. This is due to the inherent difficulty of analyzing such complex mixtures. For example the majority of the MB species have similar solubility and absorption in UV–vis–NIR region, making the direct probing of the speciation of the reaction mixture practically impossible. Recently, we demonstrated that gel electrophoresis is a powerful technique for the characterization of reaction mixtures containing POM clusters.<sup>7</sup> This is because they have a unique electrophoretic mobility depending on their size and charge (surface charge density) in solution. Initial analysis of the reaction mixture using gel electrophoresis allowed us to investigate and identify the species formed in the reaction mixture.

In this paper, we present our investigations into the MB reaction mixture as a function of pH and reagents ratio ( $R$ ) and map the reaction coordinates that define and control the system. The extent of reduction on the metal centers as well as the pH of the reaction mixture and type of counterion is crucial for the formation of either MB species or a variety of other anionic clusters, as we confirmed by gel electrophoretic chromatography and ESI-MS studies. Thus, mapping the parameter space in respect of experimental variables such as pH,  $R$ , solvent medium, and counterion effects, we identified the formation of species ranging from nanostructured MB wheels to molecular capsules  $[(\text{SO}_3)_2\text{Mo}_2\text{Mo}_{16}\text{O}_{54}]^{6-}$  ( $=\{\text{S}_2\text{Mo}_{18}\}$ ) and hexameric anionic  $[(\mu_6\text{-SO}_3)\text{Mo}_6\text{O}_{15}(\mu_2\text{-SO}_3)_3]^{8-}$  ( $=\{\text{S}_4\text{Mo}_6\}$ ) clusters. The interplay of Lewis basicity of the heteroatom present and its ability to template the self-

assembly of building blocks proved crucial for the isolation of specific products. Experimental observations suggest: (a) strong Lewis base behavior of the anionic species, (b) a lower oxidation state of Mo, and (c) low polarity of the solvent medium favors the templated self-assembly process. For example, use of  $\text{SO}_3^{2-}$  as a template (originating from the oxidation of the reductant  $\text{Na}_2\text{S}_2\text{O}_4$ ) allowed us to isolate a Dawson-like  $\{\text{S}_2\text{Mo}_{18}\}$  and a hexameric anionic species  $\{\text{S}_4\text{Mo}_6\}$  in the presence of mixed solvent system (acetonitrile–water) and tetrabutylammonium (TBA) cations. This observation allowed us to develop a new synthetic approach for the design of new types of clusters. Based on the above approach, the use of  $\text{SO}_3^{2-}$  and phenylphosphonate anions in a mixed solvent system allowed the isolation of new molecular capsule  $(\text{TBA})_5[\text{Na}(\text{SO}_3)_2(\text{PhPO}_3)_4\text{Mo}_4\text{Mo}_{14}\text{O}_{49}] \cdot n\text{MeCN}$  (**1**), where the sulfite anions occupy the interior cavities and the external surface is decorated by four phosphonate ligands. This cluster itself represents a new archetype.

## 2. RESULTS AND DISCUSSION

**2.1. Mo-Blue and Mo-Brown.** The system was investigated as a function of pH and the ratio of the starting materials ( $R = [\text{S}_2\text{O}_4^{2-}]/[\text{MoO}_4^{2-}]$ ).

A series of reaction mixtures under different experimental conditions of pH (1–4) and  $R$  (0.07, 0.14, 0.23, 0.56 and 0.90) were characterized by UV–vis–NIR spectroscopy (Figure S1–1 to S1–5). The MB species have typical absorption bands around 600–1100 nm which are attributed to the intervalence charge transfer (IVCT). Similar bands were observed for all the combinations of experimental conditions (pH,  $R$ ) except from the sets (3, 0.90) and (4, 0.56–0.90). Under these experimental conditions the reactions mixtures appeared to be brown instead of blue due to the higher amount of reducing agent, which lead to the formation of Mo-brown species.<sup>1</sup> The UV–vis–NIR data allowed us to identify the areas of the parameter space that lead to the formation of MB and Mo-brown species [(3, 0.90) and (4, 0.56–0.90)] (Figure 2). The area of the parameter space

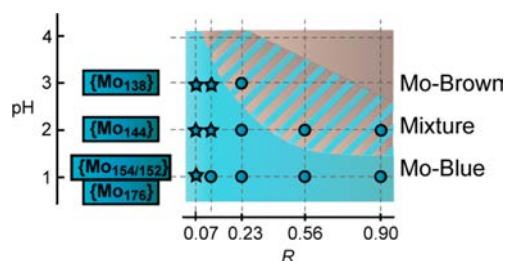


**Figure 2.** Diagram of MB and Mo-brown formed in solution after at least 24 h. Circles and stars show the conditions that yield MB wheels, but conditions that lead to single crystals are denoted by the stars.

which favors the formation of Mo-brown species was partially contaminated with MB species as confirmed by chromatographic gel electrophoresis (see below for further details). After leaving the reaction mixtures to stand at room temperature for 3 days, single crystals were obtained from the (1, 0.07) and (2, 0.07–0.14) reaction sets. Single crystal X-ray diffraction (XRD) analysis revealed two cluster types within the reaction mixture at (1, 0.07):  $\text{Na}_{15}\{\text{Mo}_{154/152}\} \cdot \text{ca. } 400\text{H}_2\text{O}$  and  $\text{Na}_{16}[\text{Mo}_{176}\text{O}_{528}\text{H}_{16}(\text{H}_2\text{O})_{80}]^{16-} \cdot \text{ca. } 450\text{H}_2\text{O}$  ( $[\text{Mo}_{176}\text{O}_{528}\text{H}_{16}(\text{H}_2\text{O})_{80}]^{16-} = \{\text{Mo}_{176}\}$ ).<sup>8</sup> From the reaction set (2, 0.07–0.14), single crystals of

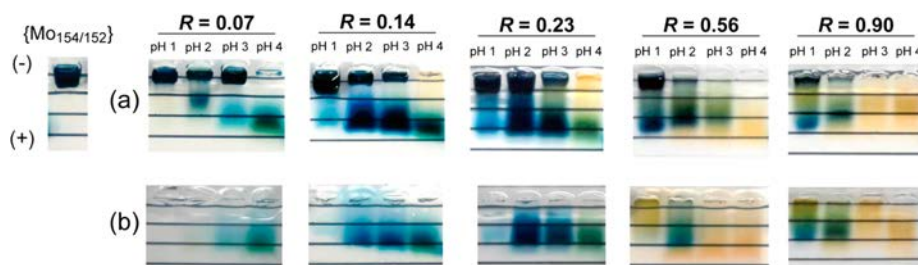


**Figure 3.** Photographs of the gels taken after electrophoresis of the (a) filtrates, from the reaction mixture, and (b) after treatment with TEAH (after stirring for 10 min). The blue bands shown in (b) that have the slowest mobility were less intense compared with the initial solutions shown in (a). On the LEFT side comparison of the mobility of the blue band with  $\{\text{Mo}_{154/152}\}$  indicate separation of MB wheels.

$\text{Na}_{24}\{\text{[Mo}_{144}\text{O}_{437}\text{H}_{14}(\text{H}_2\text{O})_{56}]_{0.5}[\text{Mo}_{144}\text{O}_{437}\text{H}_{14}(\text{H}_2\text{O})_{60}]_{0.5}\} \cdot 350\text{H}_2\text{O}$  ( $= \{\text{Mo}_{144}\}$ )<sup>9</sup> were obtained. Finally, the reaction sets (3, 0.07–0.14) gave single crystals after 24 h when treated with ammonium chloride. The cluster was crystallographically identified as  $[\text{Mo}_{138}\text{O}_{410}(\text{OH})_{20}(\text{H}_2\text{O})_{46}]^{40-}$  ( $= \{\text{Mo}_{138}\}$ ).<sup>10</sup>

**2.2. Chromatographic Gel Electrophoresis and Mass Spectrometry Analysis of Reaction Solutions.** Although reaction sets (1–3, 0.07) and (2–3, 0.14) gave single crystals, it was possible to identify the species in solution in the other collected batches using gel electrophoresis. Figure 3 shows the photograph of gels taken after the electrophoresis of the reaction mixtures after 1 day of reaction. The reaction set (1, 0.07) gave a single blue band, implying there is only a single product attributable to a MB species. The reaction conditions used are consistent with the synthesis of the  $\{\text{Mo}_{154/152}\}$  anions. (The MB wheel,  $\{\text{Mo}_{154/152}\}$ , was synthesized from a  $\text{Na}_2\text{MoO}_4$  aqueous solution in the presence of  $\text{Na}_2\text{S}_2\text{O}_4$  reducing agent at  $\text{pH} \approx 1$ , yielding blue crystals after 2 days.)

On the other hand, solutions from the reaction mixtures that did not crystallize were separated into several bands corresponding to species with different electrophoretic mobility and colors (blue, green and brown). As such, we revealed that Mo-brown was a contaminant in reactions (4, 0.14), (3–4, 0.23), (2–4, 0.56), and (2–4, 0.90).

Mass spectrometry of several reaction sets revealed very complex spectra with multiple complex envelopes that show a wide isotopic distribution, as expected for large MB anions. One of the key issues is that the MB clusters may easily reorganize and decompose under the conditions of electrospray mass spectrometry. However, despite this we were able to find three types of cluster anions:  $[\text{Mo}_4^{\text{VI}}\text{O}_{13}\text{Na}]^-$ ,  $[\text{Mo}_4^{\text{VI}}\text{O}_{14}\text{H}_7]^-$ , and  $[\text{Mo}_4^{\text{VI}}\text{O}_{13}\text{H}]^-$  could be assigned (Figure 4). These cluster anions have been observed as building blocks that exist in reaction systems.<sup>11</sup> Most of other species could not be assigned to known cluster types. We tentatively suggest that these species contain other building blocks or fragments of clusters that possess mixed valence state molybdenum centers, as

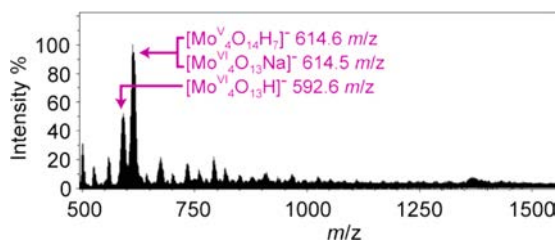


**Figure 4.** ESI-MS spectrum of solution reacted at (3, 0.14) of reaction solutions after 24 h.

suggested by IVCT signals in UV–vis–NIR spectra. Our mass spectrometry analysis of the reaction solutions indicated that (a) the reactions did not yield a single type of clusters and (b) the reaction solutions contain mixtures of clusters including building blocks and fragments that have not been isolated as crystalline forms. In this work we are interested in the relative differences as a function of the reaction conditions. Further exploration will be done not only with ESI-MS but also with a variety of corroborative techniques, while carefully monitoring the redox stability of the solutions.

**2.3. Construction of Reaction Diagrams of MB Wheels.** Isolation of MB material was achieved by the reaction with TEAH chloride. Upon treatment with TEAH chloride, a blue precipitate was immediately observed from reactions (1–3, 0.07–0.23) and (1–2, 0.56–0.90). The IR spectra of these blue powders showed a Mo–O–Mo vibration at around 900–500  $\text{cm}^{-1}$ , and they were similar to  $\{\text{Mo}_{154/152}\}$  anions (Figure S4–1 to S4–5). Figure 3b shows a photograph of the gel after the electrophoresis of filtrates of the reaction mixtures treated with TEAH. All the blue bands that had the slowest mobility in the initial filtrates seen in reactions (1–3, 0.07–0.23) and (1–2, 0.56–0.90) had disappeared, showing isolation of MB wheels as TEAH salts. The mobility and IR data suggest that the MB wheels are formed in reactions (1–3, 0.07–0.23) and (1–2, 0.56–0.90) as shown in Figure 2. In addition, Ozeki reported that the pH of the reaction influences the nuclearity of the isolated MB wheels. In general, higher pH values increase the number of defect sites on the rim of the MB wheels.<sup>10</sup> As mentioned before, we also isolated  $\{\text{Mo}_{144}\}$  and  $\{\text{Mo}_{138}\}$  anions from reactions at pH 2 and 3 ( $R = 0.07$ –0.14), respectively, showing a similar tendency as a function of the pH value.

**2.4. Triggering Template Reactions from the Building Block Mixture.** By focusing on the isolation of the building blocks, several sets of reactions yielded blue precipitates after treatment with TBA (apart from (3, 0.90) and (4, 0.56–0.90)). Recrystallization from acetonitrile yielded single crystals which were identified as the TBA salt of  $[\text{Mo}_2^{\text{V}}\text{Mo}_{16}^{\text{VI}}\text{O}_{54}(\text{SO}_3)_2]^{6-}$  ( $\{\text{S}_2\text{Mo}_{18}\}$ )<sup>12</sup> by single crystal XRD analysis. This Dawson-like cluster has been reported earlier<sup>12</sup> in agreement with the employed reaction conditions (4, 0.07) (while the concentration of  $\text{MoO}_4^{2-}$  differs). A diagram in which  $\{\text{S}_2\text{Mo}_{18}\}$  was obtained is shown in Figure 5a.

Further, an increase of the pH and  $R$  parameters yielded orange crystals of the  $[(\mu_6\text{-SO}_3)\text{Mo}_6^{\text{V}}\text{O}_{15}(\mu_2\text{-SO}_3)_3]^{8-}$  ( $\{\text{S}_4\text{Mo}_6\}$ ) anion after 2 weeks.<sup>13</sup> The parameter space scanned for the isolation of the hexameric cluster is shown in Figure 5b. The synthesis was reported using hydrazine and  $(\text{NH}_4)_2\text{SO}_3$  as a reductant and template source, respectively. Large amount of

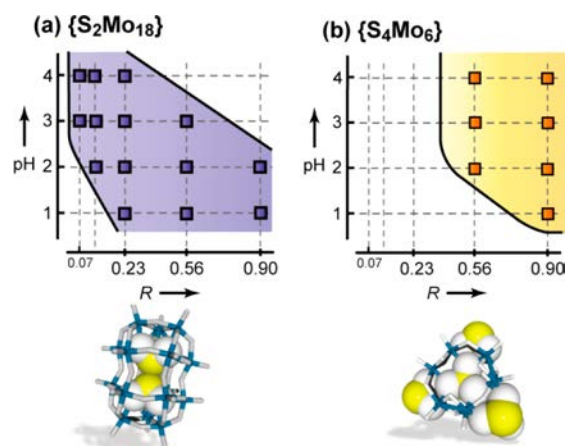


**Figure 5.** Diagrams and structures of  $\{S_2Mo_{18}\}$  and  $\{S_4Mo_6\}$  clusters (Mo: blue, O: white, S: yellow. Mo-oxide frameworks were represented by stick model with large spheres of  $SO_3^{2-}$ ). Squares show the conditions that yield each cluster.

$SO_3^{2-}$  ( $[SO_3^{2-}]/[Mo] = 5.3$ ) was required for the reaction to take place at pH = 5.5.

Interestingly, both  $\{S_2Mo_{18}\}$  and  $\{S_4Mo_6\}$  clusters were not identified by the mass spectra shown above, indicating that their self-assembly was triggered by the addition of TBA and acetonitrile after which the sulphite anion acted as template. Also, the countercation can play an important role and affect the self-assembly process.<sup>14</sup> Additionally, degradation of large species in solution giving rise to the formation of other species is also known, for example, the fragmentation of the  $\{Mo_{132}\}$ -type gigantic cluster was observed following treatment with  $[Cu(MeCN)_4]PF_6$ , which triggered the assembly of the inverse Keggin structure,  $[Mo_{12}O_{46}(PF_4)]^{4-}$ .<sup>15</sup>

**2.5. Template Reactions of Oxoanions.** It has long been known that  $XO_m^{n-}$  type oxoanions can act as templates in reactions, forming hetero-POMs. An important parameter which affects the ability of an anion to act as template is its Lewis basicity. The basic strength is correlated to the capacity

of attracting protons. Thus, the basicity, that is, the  $pK_a$  value of the corresponding anions, is correlated to the capacity to attract and interact with cationic species.

The Lewis base strength can be estimated from bond valence consideration as  $S_b$  and the values found to be in good agreement with the  $pK_a$  values of the specific anion ( $pK_a = 14.3 \ln(S_b/0.135)$ ).<sup>16</sup> Table 1 summarizes the  $pK_a$  and  $S_b$  values of different anions that were used as templates for the synthesis of hetero-POMs. Treatment of the reaction mixtures with TBA·Br and recrystallization of the obtained solid from acetonitrile, lead to the formation of single crystals.

Reactions that exploit the template effect that different heteroatoms have on the formation of hetero-POM type MB clusters are used for routine colorimetric determinations of phosphates, silicates and arsenates. This originates from the high reactivity of these template anions toward the formation of hetero-POMs.<sup>17</sup> These oxoanions tend to have a high Lewis base strength and react readily with molybdate precursor in aqueous solution.

In contrast, hetero-POM encapsulating anions that are poor Lewis bases tend to be synthesized from mixed solvent systems and/or reducing conditions. In the case of the  $ClO_4^-$  anion, which has the lowest base strength in the table, both a nonaqueous system and reducing conditions were required. This tendency indicates that mixed solvents and reducing conditions enhance reactivity. From bond valence considerations, the  $S_b$  of each template anion was estimated. In a model reaction with  $SO_3^{2-}$  as the template reacting with molybdate ions, the charge of Mo ions and Lewis base strength of O linked to S were denoted by  $m$  and  $S_b$ , respectively. The  $S_b$  is estimated as  $2 - m/3$ . With a decrease in oxidation state (charge,  $m$ ) of Mo from 6 to 5,  $S_b$  is increased from zero to 0.17 (Figure S9–1).

This shows that the template reaction is easier under the reducing conditions and indicates that MB reactions are intrinsically predisposed to take part in templated self-assembly reactions.

**Table 1.**  $pK_a$  Values and Lewis Base Strength<sup>a</sup> ( $S_b$ ) of Corresponding Anion of Oxoacid Summarized with Reaction Solvent for Synthesis of Hetero Polyoxometalate Clusters

anion	$pK_a^b$	$S_b$	hetero-POM	reaction solvent	ref
$SiO_4^{4-c}$	~10	0.33	$[(SiO_4)(MoO_3)_{12}]^{4-}$	water	19
$PO_4^{3-}$	12.3	0.25	$[(PO_4)(MoO_3)_{12}]^{3-}$	water	20
$AsO_4^{3-}$	11.5	0.25	$[(AsO_4)(MoO_3)_{12}]^{3-}$	water	20, 21
			$[(AsO_4)_2(MoO_3)_{18}]^{6-}$	water	
$B(OH)_4^-$	9.23	—	$[(BO_4)(WO_3)_{12}]^{5-}$	water	20
$P_2O_7^{4-}$	9.25	0.22	$[(P_2O_7)(MoO_3)_{18}]^{4-}$	water/acetonitrile	22
$SeO_3^{2-}$	8.3	0.22	$[Mo_{12}V_{10}O_{58}(SeO_3)_8]^{10-}$	water	23
$TeO_3^{2-}$	8.0	0.22	$[Te_3W_{21}O_{75}]^{12-}$	water	24
$SO_3^{2-}$	7.00	0.22	$[(SO_3)_2(MoO_3)_{18}]^{4-}$	water/acetonitrile	12, 25
			$[(SO_3)_2W_{18}O_{62}]^{4-}$	water/acetonitrile	
			$[(SO_3)_2(Mo^VO_3)_2(Mo^VI O_3)_{16}]^{6-}$	water	
$MoO_4^{2-}$	3.89	0.17	—	—	—
$SO_4^{2-}$	1.9	0.17	$[(SO_4)(MoO_3)_{12}]^{2-}$	water/acetonitrile	26
			$[(SO_4)_2(MoO_3)_{18}]^{4-}$	water/acetonitrile	
			$\{Mo_{368}\}^d$	water	
$ClO_4^-$	−10	0.08	$[(ClO_4)_2(W^VO_3)(W^VI O_3)_{17}]^{3-}$	DMF/acetic anhydride	27

<sup>a</sup> $pK_a$  is correlated with  $S_b$ ;  $pK_a = 14.3 \ln(S_b/0.135)$  (see ref 16). <sup>b</sup> $pK_a$  values see ref 28. <sup>c</sup>Since the anion has not been isolated, shown in the table for comparison. <sup>d</sup> $\{Mo_{368}\} (= [H_x Mo_{368} O_{1032} (H_2O)_{240} (SO_4)_{48}]^{148-})$  (see ref 26c; the moiety is a mixed valence cluster where  $SO_4^{2-}$  anions are ligated to the Mo centres).

**2.6. Reaction with Phenylphosphonate.** To exploit this understanding, we employed phenylphosphonate ( $\text{PhPO}_3^{2-}$ ) to explore the formation of a new cluster type. This is because the anion has similar Lewis base strength ( $\text{p}K_{\text{a}1}$  1.86,  $\text{p}K_{\text{a}2}$  7.51) to  $\text{SO}_3^{2-}$ , and we postulate that the steric hindrance induced by the phenyl moiety can disturb the template reaction.<sup>18</sup> Therefore, to an aqueous solution of  $\text{Na}_2\text{MoO}_4 \cdot 2\text{H}_2\text{O}$  (12.6 mmol), we added hydrochloric acid (32%) and  $\text{Na}_2\text{S}_2\text{O}_4$  phenylphosphonic acid (3 mmol). Into the aqueous solutions, 10 mL of acetonitrile was added under continuous stirring (for 30 min). The addition of TBA·Br was followed by recrystallization from acetonitrile. Several sets of reactions (1–2, 0.14–0.18) yielded blue precipitates where single crystals that are suitable for XRD analysis were obtained from the reaction (1, 0.14). Figure 6 shows the structure of the isolated

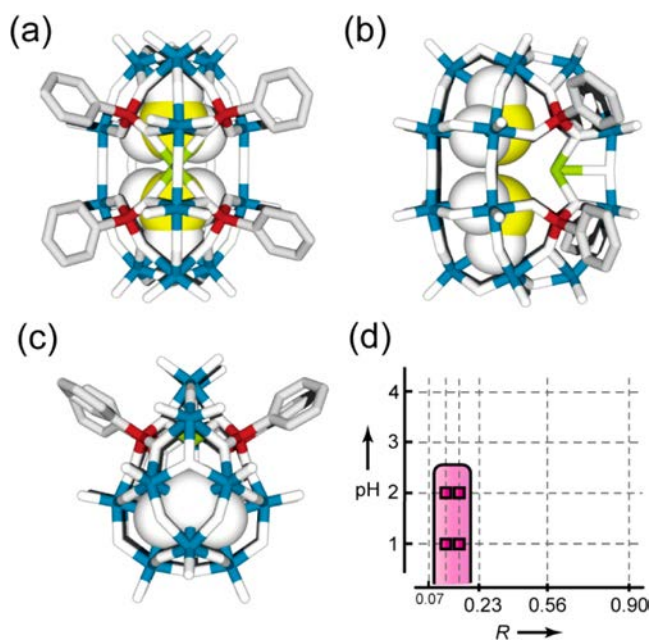


**Figure 6.** (a–c) Structure of  $[\text{Na}(\text{SO}_3)_2(\text{PhPO}_3)_4\text{Mo}_4\text{Mo}^{\text{VI}}_{14}\text{O}_{49}]^{5-}$  anion from different viewing directions with stick models in which  $\text{SO}_3^{2-}$  anions were highlighted by large ball representation (Mo, blue; O, white; P, red; C, gray; Na, green; S, yellow). H atoms were omitted. (d) Diagram of the compound 1 (pH before adding acetonitrile). Squares show the conditions that yielded the clusters.

cluster and the relevant parameter space diagram. The cluster comprises of 18 Mo ions templated internally with two  $\text{SO}_3^{2-}$  anions, resembling a  $\{\text{S}_2\text{Mo}_{18}\}$ , however, the outer shell is coordinated by four  $\text{PhPO}_3^{2-}$  anions which are attached to the cluster surface through Mo–O–P bonds and a sodium ion is encapsulated within the cluster. UV–vis–NIR spectra show IVCT bands at 688 and 1050 nm, indicating a mixed valence state between  $\text{Mo}^{\text{V}}$  and  $\text{Mo}^{\text{VI}}$  (Figure S6–2). Redox titrations (Figure S7–4) revealed that four of the 18 Mo are reduced to  $\text{Mo}^{\text{V}}$  and the cluster can be formulated as  $(\text{TBA})_5[\text{Na}(\text{SO}_3)_2(\text{PhPO}_3)_4\text{Mo}_4\text{Mo}^{\text{VI}}_{14}\text{O}_{49}] \cdot n\text{MeCN}$  (**1**) ( $2 \geq n$ ).

A reaction of acidified molybdate with the  $\text{S}_2\text{O}_4^{2-}$  reductant yields a MB wheel cluster at low pH and  $R$ . However, with increasing pH and  $R$ , the reaction gives a mixture of building blocks containing  $\text{SO}_3^{2-}$ . As the pH or  $R$  value increases, the concentration of  $\text{SO}_3^{2-}$  and  $\text{Mo}^{\text{V}}$  in the reaction system also increases (the  $\text{SO}_3^{2-}$  forms as a result of the oxidation of the reductant  $\text{S}_2\text{O}_4^{2-}$ ).

Since  $\text{SO}_3^{2-}$  is not fully utilized as a template in the initial reaction system, treatment with TBA and acetonitrile triggers a reaction to several types of cluster anion with  $\text{SO}_3^{2-}$  anion serving as a template (Figure 7). This is illustrated by an

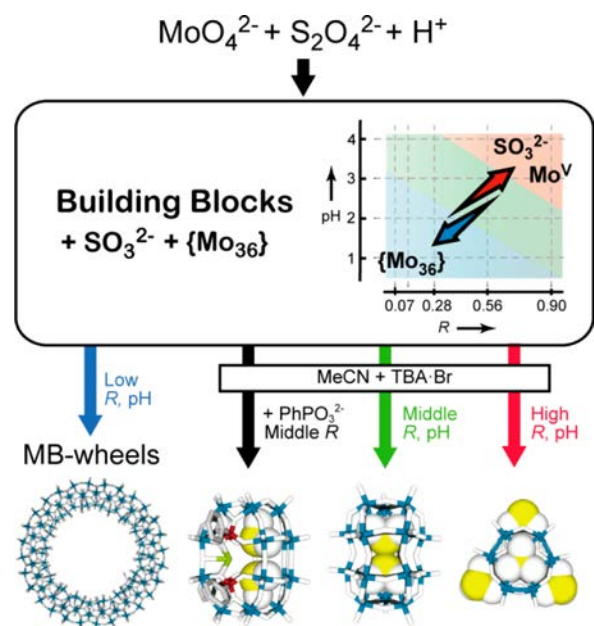


**Figure 7.** Schematic view of reaction system. S (yellow) and O (white) atoms of  $\text{SO}_3^{2-}$  are emphasized by large ball representations. Blue and white sticks correspond to Mo and O atoms, respectively.

enhancement of reactivity of the template and an encapsulation/association or “shrink-wrapping” effect. In this respect we feel these findings will lead to new methodologies for new cluster design. Further, the use of other phosphonate anions substituted with a functional organic moiety will be reported by us with details on the structure and electronic state of compound 1.

### 3. CONCLUSIONS

We have investigated the self-assembly process of MB  $\{\text{Mo}_{154/152}\}$  wheels under a range of different reaction conditions, pH (1–4) and ratio of the starting materials ( $R$ ; 0.07–0.90). UV–vis–NIR spectroscopy, gel electrophoresis, and ESI-MS not only helped us to map the reaction coordinates of the  $\text{Mo}/\text{Na}_2\text{S}_2\text{O}_4$  system but also to define the areas that favor the formation of MB and Mo-brown species. We were also able to identify the available building blocks in the reaction mixtures based on the experimental variables (pH and  $R$ ). Moreover, it was shown that not only MB wheels but also other cluster anions were present in the reaction mixtures at high pH and  $R$  values. These species were isolated by addition of TBA and acetonitrile in the aqueous reaction mixture forming  $[\text{Mo}_2\text{Mo}^{\text{VI}}_{16}\text{O}_{54}(\text{SO}_3)_2]^{6-}$  and  $[(\mu_6\text{-SO}_3)\text{Mo}_6\text{O}_{15}(\mu_2\text{-SO}_3)_3]^{8-}$  clusters revealing a relationship between the assembled architecture and the Lewis basicity of the anionic species, the extent of the reduction, and the polarity of the solvent. The interplay of template-based and redox triggered self-assembly was tested further by the cooperative effect of sulfite and phenylphosphonate anions in a mixed solvent system, in which we isolated a new molecular capsule templated by the sulphite anions and that has an external surface decorated with four phosphonate ligands. Consequently the

template driven self-assembly is favored by: (a) strong Lewis basicity of the oxoanion, (b) low oxidation state of Mo, and (c) reduced polarity of the solvent used. Our results shown here demonstrate a new design approach for the synthesis of novel clusters and the control of template triggered self-assembly.

#### 4. EXPERIMENTAL PROCEDURES

**4.1. Measurements.** IR spectra (4000–450  $\text{cm}^{-1}$ ) measurements were carried out on KBr disks with a resolution of 4  $\text{cm}^{-1}$ . All spectra are shown in Supporting Information (SI). Single-crystal XRD analysis was performed using Rigaku Mercury CCD area detector with graphite-monochromated Mo-K $\alpha$  radiation. The data were collected at 173 K to a maximum  $2\theta$  value of 55.0. The structure was determined by direct methods and expanded using Fourier techniques.

**4.2. Reactions.** Aqueous solutions of sodium molybdate (12.7 mmol, 25 mL) and sodium dithionite were reacted at different molar ratios to molybdate denoted as  $R = [\text{S}_2\text{O}_4^{2-}]/[\text{MoO}_4^{2-}]$  (0.07, 0.14, 0.23, 0.56 or 0.90), and the pH was adjusted by the addition of hydrochloric acid to pH 1, 2, 3, or 4. After 1 day of reaction in a closed flask, the filtrates (solution I) were characterized by UV–vis–NIR spectra, gel electrophoresis, and mass spectrometry.

**4.3. Isolation from Reaction Mixture by Cation Exchange Reaction.** **4.3.1. Ammonium Salt.** Solution I was treated with ammonium chloride. Single crystals were obtained from reactions (pH,  $R$ ) = (3, 0.07–0.14). The cluster type was crystallographically identified as  $[\text{Mo}_{138}\text{O}_{410}(\text{OH})_{20}(\text{H}_2\text{O})_{46}]^{40-}$ .

**4.3.2. TEAH Salt.** A similar procedure with triethanolammonium (TEAH) chloride (1.0 g) gave blue precipitates from solution I. They were characterized by using IR spectroscopy to determine the type of cluster. The TEAH salt showed spectra typical for MB wheels shown in SI. A filtrate (solution II) after separating TEAH salt was characterized using gel electrophoresis which showed that the blue band that had the slowest mobility was diminished if compared with that of solution I.

**4.3.3. TBA Salt.** Solution II was treated with tetrabutylammonium (TBA) bromide (1.0 g), yielding an immediate precipitate depending on reaction conditions. The TBA salt was recrystallized from acetonitrile giving single crystals suitable for XRD analysis and IR spectra were collected in addition (see Figures S4–6 to S4–10). They were identified to  $\{\text{S}_2\text{Mo}_{18}\}$ . If the filtrates were orange in color, single crystals could be obtained after 5–7 days by keeping flask opened. Single crystal XRD analysis and IR spectra (Figure S4–11 to S4–12) revealed that  $\{\text{S}_4\text{Mo}_6\}$  anion included in the crystal.

**4.4. Gel Electrophoresis.** The electrophoresis studies were performed using a commercially available submarine-type electrophoresis system (Pt-wire electrodes set at a distance of 13 cm). Acetic acid/sodium acetate buffer (pH 5.0) was applied, and agarose (purchased from Sigma-Aldrich and used without further purification) gels were prepared using the same buffer by cooling an agarose solution from boiling temperature. A solution was injected into slots in the gels in 15  $\mu\text{L}$  portions, and a voltage (100 V) was applied to the system for 10 min.

**4.5. Characterization of  $\{\text{S}_2\text{Mo}_{18}\}$  Anion.** The cluster type has been reported so far,<sup>12</sup> while we isolated as a TBA salt. From XRD analysis, redox titration, IR, and UV–vis–NIR spectroscopy, composition was suggested as  $\text{TBA}_5\text{H}[\text{Mo}_2^{\text{V}}\text{Mo}_{16}^{\text{VI}}\text{O}_{54}(\text{SO}_3)_2] \cdot n\text{MeCN}$ . The crystalline products were collected by filtration and dried to remove acetonitrile for elemental analysis. (Found: C, 24.48; H, 4.64; N, 1.95; Calcd for  $\text{C}_{80}\text{H}_{181}\text{Mo}_{18}\text{N}_5\text{O}_{60}\text{S}_2$ : C, 24.24; H, 4.60; N, 1.77%). UV–vis–NIR spectra (acetonitrile):  $\lambda_{\text{max}}(\text{MeCN})/\text{nm}$  801 ( $\epsilon/\text{dm}^3 \text{ mol}^{-1} \text{ cm}^{-1}$  8032) Crystal data for  $\{\text{S}_2\text{Mo}_{18}\}$  anion:  $\text{C}_{84.5}\text{H}_{186}\text{Mo}_{18}\text{N}_{7.5}\text{O}_{60}\text{S}_2$ ,  $M = 4058.45 \text{ g mol}^{-1}$ , orthorhombic,  $a = 18.0117(2)$ ,  $b = 27.2840(5)$ ,  $c = 28.0044(5) \text{ \AA}$ ,  $V = 13762.2(4) \text{ \AA}^3$ ,  $T = 173 \text{ K}$ , space group  $P2_12_12_1$  (no. 19),  $Z = 4$ , 147665 reflections measured, 31543 unique ( $R_{\text{int}} = 0.0506$ ) which were used in all calculations. The final  $R_1$  (observed data) and  $wR_2$  (all data) were 0.0666 and 0.1924, respectively. CCDC number 1037251.

**4.6. Characterization of  $\{\text{S}_4\text{Mo}_6\}$  Anion.** The anion also has been reported with different counter cations.<sup>13</sup> The orange crystals

turned opaque easily due to desorption of crystalline water, however we were able to solve the crystal structure revealing the compound as  $[(\mu_6\text{-SO}_3)\text{Mo}_6\text{O}_{15}(\mu_2\text{-SO}_3)_3]^{8-}$ , a cluster anion with several TBA cations, disordered water molecules, and sodium ion. Crystallographic data and IR spectra were included in SI.

**4.7. Synthesis and Characterization of 1.** Single crystals of the compound **1** were obtained according to the following procedure. The reaction variable is corresponded to (1, 0.18). To an aqueous solution of  $\text{Na}_2\text{MoO}_4 \cdot 2\text{H}_2\text{O}$  (12.6 mmol, 25 mL) was added, hydrochloric acid (32%, 3.0 mL),  $\text{Na}_2\text{S}_2\text{O}_4$  (2.30 mmol), phenylphosphonic acid (3 mmol), and acetonitrile (10 mL) under continuous stirring for 30 min (pH 1 before adding acetonitrile), and the filtrate was kept in a closed flask for 3 days. After filtration, TBA-Br (0.70 g) was added, and a blue precipitation was formed which was then recrystallized from acetonitrile. Blue crystals were obtained after 2–3 days. Redox titration with  $\text{Ce}^{\text{IV}}(\text{SO}_4)_2$  (0.01 N) in mixed solvent (DMSO; 5 mL, 1 M  $\text{H}_2\text{SO}_4$ ; 5 mL) showed that there are four equivalent numbers of  $\text{Mo}^{\text{V}}$ . Composition was deduced to  $(\text{TBA})_5[\text{Na}(\text{SO}_3)_2(\text{PhPO}_3)_4\text{Mo}_4^{\text{V}}\text{Mo}_{14}^{\text{VI}}\text{O}_{49}] \cdot n\text{MeCN}$  (two acetonitrile molecules are identified crystallographically, however there is void space occupied by a undetermined number of disordered solvent molecules). Yield: 1.83 g (42% based on Mo). Elemental analysis: Found: C, 27.48; H, 4.20; N, 1.48; Calcd for  $\text{C}_{104}\text{H}_{200}\text{Mo}_{18}\text{N}_5\text{NaO}_{67}\text{P}_4\text{S}_2$ : C, 27.57; H, 4.45; N, 1.55%. UV–vis–NIR spectra (acetonitrile):  $\lambda_{\text{max}}(\text{MeCN})/\text{nm}$  668, 1050. IR (KBr):  $\nu_{\text{max}}/\text{cm}^{-1}$  3446 (br), 2961 (m), 2873 (m), 2360 (w), 1635 (w), 1482 (m), 1380 (w), 1184 (m), 1146 (m), 1133 (m), 1045 (m), 1026 (m), 963 (s), 937 (s), 909 (m), 867 (w), 816 (m), 788 (m), 724 (m), 708 (m), 562 (m) (see Figure S4–13). Crystal data for **1**:  $\text{C}_{56}\text{H}_{99}\text{Mo}_9\text{N}_{4.5}\text{Na}_{0.5}\text{O}_{33.5}\text{P}_2\text{S}$ ,  $M = 2330.27 \text{ g mol}^{-1}$ , monoclinic,  $a = 33.20(2)$ ,  $b = 17.635(10)$ ,  $c = 32.189(20) \text{ \AA}$ ,  $\beta = 115.3192(18)^\circ$ ,  $V = 17033(17) \text{ \AA}^3$ ,  $T = 173 \text{ K}$ , space group  $C2/c$  (no. 15),  $Z = 8$ , 61365 reflections measured, 17768 unique ( $R_{\text{int}} = 0.1516$ ) which were used in all calculations. The final  $R_1$  (observed data) and  $wR_2$  (all data) were 0.0885 and 0.2571, respectively. CCDC number 1037252.

#### ■ ASSOCIATED CONTENT

##### Supporting Information

UV–vis–NIR spectra, chromatographic gel electrophoresis, isolation and identification of MB wheels, IR analysis, mass spectra, redox titration, structural data including CIF files, Lewis base strength from bond valence consideration, and reaction scanning for compound **1**. The Supporting Information is available free of charge on the ACS Publications website at DOI: 10.1021/ja512758j.

#### ■ AUTHOR INFORMATION

##### Corresponding Authors

\*ryotsuna@yamaguchi-u.ac.jp

\*Lee.Cronin@glasgow.ac.uk

##### Notes

The authors declare no competing financial interest.

#### ■ ACKNOWLEDGMENTS

This work was partly supported by the Grant-in-Aid for Science Research from the Ministry of Education, Culture, Sports, Science and Technology of Japan. We thank the EPSRC platform grant (no. EP/J015156/1) and programme grant (no. EP/L023652/1). L.C. thanks the Royal Society/Wolfson Foundation for a Merit Award, and we also would like to thank the University of Glasgow for funding.

#### ■ REFERENCES

- (1) (a) Müller, A.; Meyer, J.; Krickemeyer, E.; Diemann, E. *Angew. Chem., Int. Ed. Engl.* **1996**, *35*, 1206–1208. (b) Müller, A.; Roy, S. *Coord. Chem. Rev.* **2003**, *245*, 153–166. (c) Müller, A.; Serain, C. *Acc.*

*Chem. Res.* **2000**, *33*, 2–10. (d) Baker, L. C. W.; Glick, D. C. *Chem. Rev.* **1998**, *98*, 3–49.

(2) (a) Song, Y.-F.; Tsunashima, R. *Chem. Soc. Rev.* **2012**, *41*, 7384–7402. (b) Long, D.-L.; Tsunashima, R.; Cronin, L. *Angew. Chem., Int. Ed.* **2010**, *49*, 1736–1758.

(3) Müller, A.; Das, S. K.; Fedin, V. P.; Krickemeyer, E.; Beugholt, C.; Bögge, H.; Schmidtman, M.; Hauptfleisch, B. *Z. Anorg. Allg. Chem.* **1999**, *625*, 1187–1192.

(4) (a) Liu, T.; Diemann, E.; Li, H.; Dress, A.W. M.; Müller, A. *Nature* **2003**, *426*, 59–62. (b) Liu, T. *Langmuir* **2010**, *26*, 9202–9213.

(5) (a) Noro, S.; Tsunashima, R.; Kamiya, Y.; Uemura, K.; Kita, H.; Cronin, L.; Akutagawa, T.; Nakamura, T. *Angew. Chem., Int. Ed.* **2009**, *48*, 8703–8706. (b) Imai, H.; Akutagawa, T.; Kudo, F.; Ito, M.; Toyoda, K.; Noro, S.; Cronin, L.; Nakamura, T. *J. Am. Chem. Soc.* **2009**, *131*, 13578–13579. (c) Tsuda, A.; Hirahara, E.; Kim, Y.-S.; Tanaka, H.; Kawai, T.; Aida, T. *Angew. Chem., Int. Ed.* **2004**, *43*, 6327–6331. (d) Alam, M. A.; Kim, Y.-S.; Ogawa, S.; Tsuda, A.; Ishii, N.; Aida, T. *Angew. Chem., Int. Ed.* **2008**, *47*, 2070–2073. (e) Polarz, S.; Smarsly, B.; Antonietti, M. *ChemPhysChem* **2001**, *2*, 457–461.

(6) (a) Miras, H. N.; Cooper, G. J. T.; Long, D.-L.; Bögge, H.; Müller, A.; Streb, C.; Cronin, L. *Science* **2010**, *327*, 72–74. (b) Miras, H. N.; Richmond, C. J.; Long, D.-L.; Cronin, L. *J. Am. Chem. Soc.* **2012**, *134*, 3816–3824.

(7) Tsunashima, R.; Richmond, C.; Cronin, L. *Chem. Sci.* **2012**, *3*, 343–348.

(8) Müller, A.; Merca, A.; Al-Karawi, A. J. M.; Garai, S.; Bögge, H.; Hou, G.; Wu, L.; Haupt, E. T. K.; Rehder, D.; Haso, F.; Liu, T. *Chem.–Eur. J.* **2012**, *18*, 16310–16318.

(9) Müller, A.; Krickemeyer, E.; Bögge, H.; Schmidtman, M.; Beugholt, C.; Das, S. K.; Peters, F. *Chem.–Eur. J.* **1999**, *5*, 1496–1502.

(10) Shishido, S.; Ozeki, T. *J. Am. Chem. Soc.* **2008**, *130*, 10588–10595.

(11) (a) Wilson, E. F.; Abbas, H.; Duncombe, B. J.; Streb, C.; Long, D.-L.; Cronin, L. *J. Am. Chem. Soc.* **2008**, *130*, 13876–13884. (b) Rosnes, M. H.; Yvon, C.; Long, D.-L.; Cronin, L. *Dalton Trans.* **2012**, *41*, 10071–10079.

(12) Long, D.-L.; Kögerler, P.; Cronin, L. *Angew. Chem., Int. Ed.* **2004**, *43*, 1817–1820.

(13) Manos, M. J.; Woollins, J. D.; Slawin, A. M. Z.; Kabanos, T. A. *Angew. Chem., Int. Ed.* **2002**, *41*, 2801–2805.

(14) Pradeep, C. P.; Long, D.-L.; Cronin, L. *Dalton Trans.* **2010**, *39*, 9443–9457.

(15) Fielden, J.; Quasdorf, K.; Cronin, L.; Kögerler, P. *Dalton Trans.* **2012**, *41*, 9876–9878.

(16) Brown, I. D. In *Structure and Bonding in Crystals*; O’Keeffe, M., Navrotsky, A., Eds.; Academic Press: New York, 1981; Vol. 2, pp 1–30.

(17) (a) Woods, J. T.; Mellon, M. G. *Ind. Eng. Chem., Anal. Ed.* **1941**, *13*, 760–764. (b) Clausen, D. F.; Shroyer, J. H. *Anal. Chem.* **1948**, *20*, 925–926.

(18) Nagarajan, K.; Shelly, K. P.; Perkins, R. P.; Stewart, R. *Can. J. Chem.* **1987**, *65*, 1729–1733.

(19) Strickland, J. D. H. *J. Am. Chem. Soc.* **1952**, *74*, 862–867.

(20) Deltcheff, C. R.; Fournier, M.; Franck, R.; Thouvenot, R. *Inorg. Chem.* **1983**, *22*, 207–216.

(21) Ichida, H.; Sasaki, Y. *Acta Crystallogr., Sect. C: Struct. Chem.* **1983**, *39*, 529–533.

(22) Himeno, S.; Saito, A.; Hori, T. *Bull. Chem. Soc. Jpn.* **1990**, *63*, 1602–1606.

(23) Corella-Ochoa, M. N.; Miras, H. N.; Long, D.-L.; Cronin, L. *Chem.–Eur. J.* **2012**, *18*, 13743–13754.

(24) Gao, J.; Yan, J.; Beeg, S.; Long, D.-L.; Cronin, L. *Angew. Chem., Int. Ed.* **2012**, *51*, 3373–3376.

(25) Long, D.-L.; Abbas, H.; Kögerler, P.; Cronin, L. *Angew. Chem., Int. Ed.* **2005**, *44*, 3415–3419.

(26) (a) Hori, T.; Tamada, O.; Himeno, S. *J. Chem. Soc., Dalton Trans.* **1989**, 1491–1497. (b) Hori, T.; Himeno, S.; Tamada, O. *J. Chem. Soc., Dalton Trans.* **1996**, 2083–2087. (c) Müller, A.; Botar, B.;

Das, S. K.; Bögge, H.; Schmidtman, M.; Merca, A. *Polyhedron* **2004**, *23*, 2381–2385.

(27) Zhu, S.-S.; Yue, B.; Shi, X.-Q.; Gu, Y.-D.; Liu, J.; Chen, M.-Q.; Huang, Y.-F. *J. Chem. Soc., Dalton Trans.* **1993**, 3633–3634.

(28) (a) Kolthoff, I. M. *Treatise on Analytical Chemistry*; Interscience Encyclopedia, Inc.: New York, 1959. (b) Brownstein, S.; Stillman, A. E. *J. Phys. Chem.* **1959**, *63*, 2061–2062. (c) Hildebrand, J. H. *Principles of Chemistry*; The Macmillan Company: New York, 1940. (d) Bjerrum, J.; Schwarzenbach, G.; Sillen, L. G. *Stability Constants*; Chemical Society: London, 1958. (e) Cruywagen, J. J. *Adv. Inorg. Chem.* **1999**, *49*, 127–182.